# Nanoscale

Accepted Manuscript


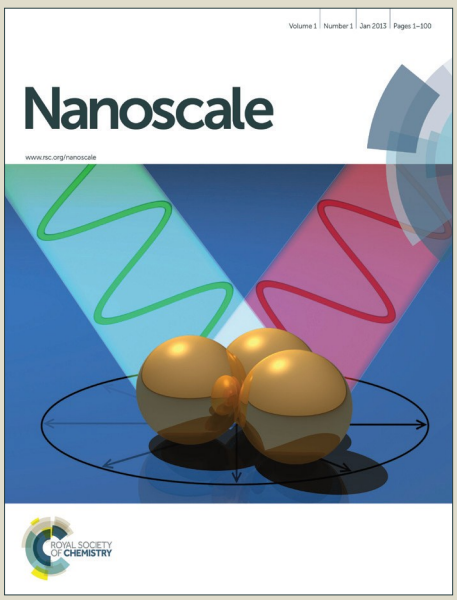





ROYAL SOCIETY OF CHEMISTRY

www.rsc.org/nanoscale

Journal Name

RSCPublishing

ARTICLE

# Supramolecular Fabrication of Multilevel Graphene-based Gas Sensors with High $NO_2$ Sensibility

Cite this: DOI: 10.1039/xoxxoooooox

Zhuo Chen,[1,a] Ahmad Umar,[b] Yao Wang,[*,a] Tong Tian,[a] Ying Shang,[a] Yuzun Fan,[a] Qi Qi,[c] Dongmei Xu,[c] and Lei Jiang[a,d]

Received ooth January 2012,
Accepted ooth January 2012

DOI: 10.1039/xoxxoooooox

www.rsc.org/

This paper reports the supramolecular assembly of silver nanoparticles- naphthalene-1-sulphonic acid-reduced Graphene Oxide (Ag-NA-rGO) and their utilization to fabricate highly sensitive and selective gas sensor. The prepared supramolecular assembly acted not only as non-covalent functionalization platform (π–π interaction) but also exhibited as an excellent scaffold to fabricate highly sensitive and selective low concentration $NO_2$ gas sensor. The prepared composites were characterized using several techniques which revealed that the graphene sheets were dispersed as ultrathin monolayers with the uniformly distribution of silver nanoparticles. The fabricated multilevel structure exhibited an excellent sensing performance, i.e. 2.8 times better, towards 10 ppm $NO_2$ compared to the NA-rGO and rGO based sensors. Apart from the high sensitivity, superior reversibility and selectivity, the prepared supramolecular assembly exhibited outstanding linear response over the large concentration range from 1ppm to 10 ppm. The presented results demonstrate that the prepared supramolecular assembly holds a great potential to fabricate efficient and effective low-concentration $NO_2$ gas sensors for practical applications.

## Introduction

Recently, graphene has attracted much attention due to its unique and outstanding characteristics such as high surface area, excellent electrical conductivity and mechanical flexibility, high thermal and chemical stabilities, etc, special structure and specific surface properties.[1-4] Since, Geim and Novoselov[1] successfully exfoliated graphene from graphite, the graphene, a single layer of carbon atoms with honeycomb crystal lattice, has guided new directions not only in the areas of electronics, optoelectronics and energy but also in sensors and biological applications due to its unique two-dimensional sp2-bonded structure.[2, 3, 5-8] Two most fascinating properties of graphene are the carrier-density dependent electrical conductivity and exceptionally high electron mobilities.[9, 10] The excellent properties of graphene are due to its unique band structure which exhibits conduction and valence bands with near-linear dispersion that touch at the Brillouin zone corners to form a zero band-gap semiconductor.[11]

Because of the unique structure and exotic properties, recently, graphene and its based composites are considered as promising materials for gas sensing applications.[12-14] Therefore, the functionalized graphene materials provide perfect 2D platform with exceptional electronic properties for interactions between the external molecules (gaseous, chemicals, etc) and the functionalized groups on the modified graphene surface.[15] Thus, with such interactions, the electronic properties of materials change, which are the key factors to explain the sensing mechanisms of the graphene based sensors. For instance, the performances of the graphene based gas sensors can be estimated by observing the variations in the electrical conductivity which changes upon the adsorption of gaseous molecules on the graphene surfaces. The adsorbed molecules change the local carrier concentration in graphene, which leads to step-like changes in resistance.[11] However, for practical gas sensing applications based on graphene or its composites, there are two important aspects which should be addressed, i.e. improve the dispersibility in solution[16, 17] and enhance the electronic properties at the solid state[18].

To improve the dispersibility and sensibility, the graphene oxide (GO) was chemically modified by functionalizing it with certain functional groups, via covalent bonding, such as sulfophenyl which has electron-withdrawing ability.[19] Although covalently bonded fucntionalized graphene-based materials can demonstrate good sensing performance, the original perfect atomic lattice of graphene would be potentially sacrified by the subsequently formed convalent bonds during chemical modification process which severely affects the intrinsic electrical properties of graphene. As a result, the electrical properties of graphene-based gas sensing materials would be significantly decreased. Moreover, covalently chemical modification usually requires strict reaction conditions with complex chemical reaction processes and of course relative high cost which restricted the widespread commercial application.[11]

Thus, to overcome such disadvantages of graphene, the strategy of supramolecular assembly based on non-covalent interactions such as electrostatic forces, hydrogen bonding, π-π stacking, hydrophobic interaction etc, is an alternative approach, by which there is no covalently bonding effect at all on the intact structure of graphene due to only non-covalent interaction taken place during the assembly.[20, 21] In addition, supramolecular assembly offers more varieties of "guest substances" (i.e.: inorganic ions, organic small molecules or macromolecules, metallic nanoparticles etc.) which can be assembled with graphene sheets.[22] Importantly, such supramolecular assembly can be prepared using facile process and at very mild temperature. Thus, we believe that the fabrication of graphene-based gas sensors using supramolecularly assembled materials is going to be a very promising research field. Further, it provides the possibility of comprehensive integration of multifunction which can stem either from "guests" or graphene ("host") or both in the assembled composites.[23-27]

Based on the above mentioned idea, this paper reports the fabrication of highly sensitive, selective and reversible $NO_2$ gas sensor based on multilevel silver nanoparticles (Ag)-naphthalene-1-sulphonic acid (NA) -reduced graphene oxide (r-GO) (Ag-NA-rGO) composite prepared via supramolecular assembly. Here, the naphthalene-1-sulphonic acid (NA) which has a large planar conjugated structure acttached with r-GO through π-π stacking and the silver nanoparticles through electrostatic forces.

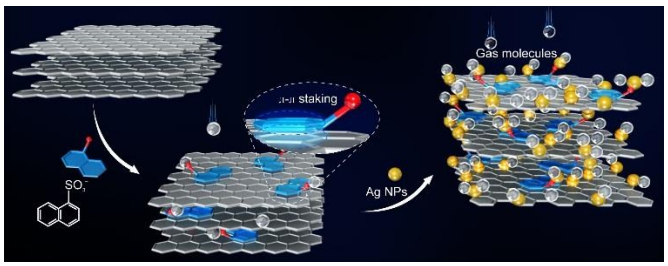


**Scheme 1.** Schematic illustration to prepare Ag-NA-rGO supramolecular assembly for $NO_2$ gas sensing applications.

In the presented work, the reduced graphene (rGO) was prepared as the one-level system (**Level I**). Further, the sulfophenyl (ph–$SO_3^-$) as a typical electron-withdrawing groups to $NO_2$ was introduced via supramolecular assembling NA with GO through π-π stacking. After situ reduction in hydrazine, a two-level (**Level II**) assembly system NA-rGO was obtained which was also used to study the $NO_2$ gas sensing characteristics. In order to further increase the adsorption capacity towards the sensing molecules,[28] silver nanoparticles were introduced in the system by electrostatic interaction as exceptional hydrophilic "guests". The prepared assembled multilayer was then situ reduced into a three-level (**Level III**) assembly system Ag-NA-rGO (**Scheme 1**).

Thus, this paper reports the fabrication and gas sensing performance of prepared all three systems, i.e. Level I: rGO; Level II: NA-rGO; and Level III Ag-NA-rGO. Interesingly, it was observed that the $NO_2$ gas sensor fabrictaed based on Level III: Ag-NA-rGO system exhibited highest gas sensing performance and a maximum response to 10 ppm $NO_2$ can reach to 2.8 times and the sensing signal linearly increases even at low concentration of $NO_2$ (1-10 ppm) in this system. Further, the effect of multilevel structure on the gas sensing performance was also systematically investigated in this work. To the best of our knowledge, this is the first ever report which demonstrates the $NO_2$ gas sensing performance of supramolecularly modified graphene. Thus, the presented work demonstrates a facile and effective approach to fabricating high-performance graphene-based materials for gas sensing applications.

## Results and Discussion

### Fabrication of the Graphene-Based Sensors

In the Level I system, the rGO was used as the basic gas sensing material which can be readily prepared after the reduction of hydrazine hydrate. GO has a regular C-C lattice which can assemble with large conjugated molecules such as benzene, naphthalene and anthracene through π-π stacking to form supramolecularly modified graphene.[29, 30]

For Level II system, a functional organic molecule NA with large planar conjugated structure was selected owing to the sulfophenyl is an electron-withdrawing group. The NA molecule comprises naphthalene ring which offers the intrinsic driving force for π–π stacking with graphene and negatively charged terminals (-$SO_3^-$) enhance hydrophilicity.[30, 31] Thus, the rGO was decorated via supramolecular modification and hence NA-rGO was prepared after the reduction process.

In Level III system, silver (Ag) nanoparticles were introduced into the Level II system via supramolecular assembly. The Ag nanoparticles were introduced in the system as another exceptional "guest" to further improve the gas sensing performance of the prepared material. Precisely, the supramolecular driving force to import the silver ions ($Ag^+$) was electrostatic interaction, by which positive charged silver ions ($Ag^+$) were assembled with the sulfophenyl (Ph-$SO_3^-$) on NA molecule and carboxylic groups (-$COO^-$) available on the GO surfaces. The major aim to incorporate the Ag nanoparticles into the system was to isolate the graphene layers for enhancing the contact areas with the targeted gaseous molecules.

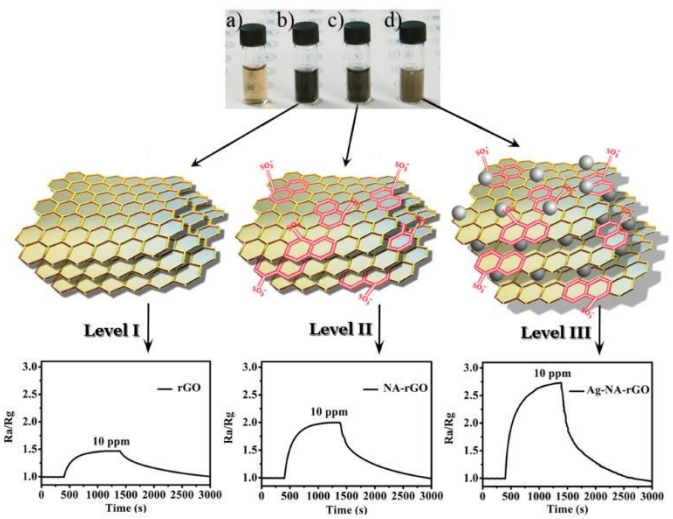


**Figure 1.** The physical picture of a) GO b)rGO c) NA-rGO and d) Ag-NA-rGO solution with the same concentration of 0.2mg/mL and the ideal corresponding supramolecular assembly structures with different sensibilities of 1.3, 2.0 and 2.8 times towards 10ppm $NO_2$ respectively.

Importantly, it is worth mentioning that the water-solubility of NA-rGO and Ag-NA-rGO composites were greatly improved for the hydrophilicity of sulfophenyl groups in NA, which well resolved the puzzle of poor dispersibility of graphene. **Figure 1** exhibits the typical physical pictures of GO, rGO, NA-rGO and Ag-NA-rGO and their ideal supramolecular assembly structures with different sensitivities towards 10 ppm $NO_2$ gas for graphene-based sensors. The GO solution color was light brownish yellow (Figure 1a); interestingly, the rGO solution color was darkened (Figure 1b) which revealed that the graphene-oxide was successfully reduced; the formed NA-rGO solution also displayed a black color (Figure 1c), while Ag-NA-rGO solution possess a dark green color (Figure 1d). Importantly, all the prepared materials exhibited different sensibilities towards 10 ppm $NO_2$ gas (Figure 1), respectively.

**Characterizations of Graphene-based sensors**

The ultrathin graphene sensing layer was deposited on the surface of a micro-grid array with pure carbon film from their dispersion (0.2 mg/mL, same concentration as gas sensing test). **Figure 2a** shows a typical transmission electron microscopic (TEM) image of a monolayer of Ag-NA-rGO. Silver nanoparticles were uniformly dispersed on graphene sheet with similar scales, ranges from 15 nm to 25 nm. Similar morphologies were also examined by atomic force microscopy (AFM) as shown in Figure S1. As evident from the AFM graph, that the graphene sheets are well dispersed and possessing ultrathin monolayers. Further, the silver nanoparticles are uniformly dispersed on the graphene sheet. According to the AFM measurement, the thicknesses of Ag-NA-rGO sheets are approximately 1-1.5 nm.

**Figure 2b** exhibits a typical scanning electron microscopic (SEM) image of a multilevel Ag-NA-rGO sheet coated on the surface of an interdigitated electrode (IE). The observed SEM image reflects the real morphology during the gas sensing test for using the same dispersion and devices. A multi-layer graphene sheets can be clearly seen together with uniformly distributed silver nanoparticles on the surface or among the layers. The multilevel structure is in conformity with the ideal supramolecular assembly structure which has originally been designed (Figure 1d).

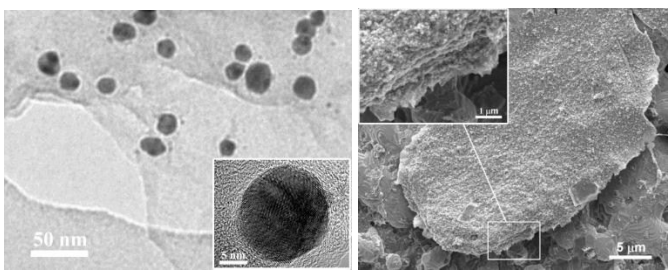


**Figure 2.** a) TEM image of a typical single layer of Ag-NA-rGO in different scales. b) SEM image of typical multilevel Ag-NA-rGO sheets deposited on the surface of an interdigitated electrode.

To examine the crystal quality and structures, rGO, NA-rGO and Ag-NA-rGO hybrid composites were investigated by X-ray diffraction (XRD) and results are shown in **Figure 3a**. The XRD pattern for rGO and NA-rGO exhibit a single diffraction reflection at 22.78°, which is attributed to the diffraction from the (002) plane of hexagonal graphite structure. The X-ray diffraction intensities of the rGO and NA-rGO composite reveal the degree of graphitization of the prepared materials. Interestingly, when the NA-rGO composite was modified with Ag nanoparticles, several new diffraction reflections are seen in the pattern which are mostly related with Ag ions. The Ag-NA-rGO composite exhibited several well-defined diffraction reflections at 2θ= 38.34°, 44.52°, 64.68° and 77.58°, attributed to the (111), (200), (220) and (311) planes, respectively which are corresponding to the face-centered cubic (fcc) structure of Ag nanoparticles[28, 32] Interestingly, a new peak appearing at 16.12° indicate that the assembled of Ag nanoparticles slightly increase the interlayer distance from 0.39 nm (2θ=22.78°) to 0.55 nm (2θ=16.12°).

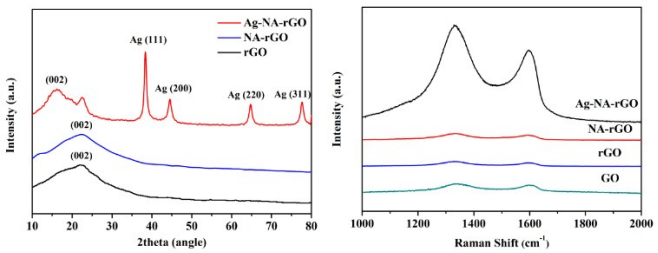


**Figure 3.** a) XRD patterns of rGO, NA-rGO and Ag-NA-rGO films and b) Raman spectrum of GO, rGO, NA-rGO and Ag-NA-rGO films.

Further, the detailed structural properties of the prepared materials were examined by Raman-scattering spectroscopy and results are shown in **Figure 3b**. The Ag-NA-rGO composite exhibits two very clear Raman-bands appearing at 1329cm$^{-1}$ and 1597cm$^{-1}$, correspond to D- and G-bands, respectively. It is well known that the intensity ratios of D- and G-bands (ID/IG) are related to the structural defects which are created by functional groups on carbon basal plane and disordered structures of graphitic domains. Theoretically, the higher ID/IG value refers to the fewer defects and possessing better structures. The ID/IG values for rGO, NA-rGO and Ag-NA-rGO were calculated and found to be 1.35, 1.34 and1.35, respectively. These calculated values are higher than that of GO (1.15) which clearly exhibiting the successful reduction of structural defects as most of the functional groups of GO were eliminated after reduction. Basically the same with rGO, the ID/IG value of NA-rGO and Ag-NA-rGO is 1.34 and 1.35 respectively, which could be attributed to the special advantages of supramolecular modification for preserving the inherent structure of graphene rather than chemical modification. The intact structure with fewer defects would directly contribute to the promotion of conductivity, which plays the key role in gas sensitivity. Table S1 summarizes the Raman shift, peak intensities and intensity ratios ($I_D/I_G$) of all four samples, i.e. Ag-NA-rGO, NA-rGO, rGO and GO.

To investigate the surface properties, the prepared rGO, NA-rGO and Ag-NA-rGO were further characterized by X-ray photoelectron spectroscopy (XPS). As shown in Figure 4, XPS spectra exhibit the existence of elemental Ag and the elemental status of Ag (3d). The Ag (3d) peaks are a doublet which arises from spin−orbit coupling ($3d_{5/2}$ and $3d_{3/2}$).[33] The binding

energies of Ag $3d_{5/2}$ and Ag $3d_{3/2}$ peaks are observed at 368.9 and 375 eV, respectively. The orbital interaction splitting of the 3d doublet of Ag was 6.0 eV and the typical binding energy values (the standard binding energy of Ag $3d_{5/2}$ for bulk Ag is about 368.2 eV), suggesting the formation of metallic silver. Besides, the asymmetric shape of the peaks also indicates the metallic silver rather than silver oxide.[34] Moreover, we can further confirm the metallic silver does exist in Ag-NA-rGO composites through the XRD analysis. Besides, it can be proved from the observed spectrum that the NA is making complex with the graphene by supramolecular modification. Further, quantitative analysis indicates that the proportions of carbon in the three sensing materials were 66.2%, 44.1% and 17.2% respectively,

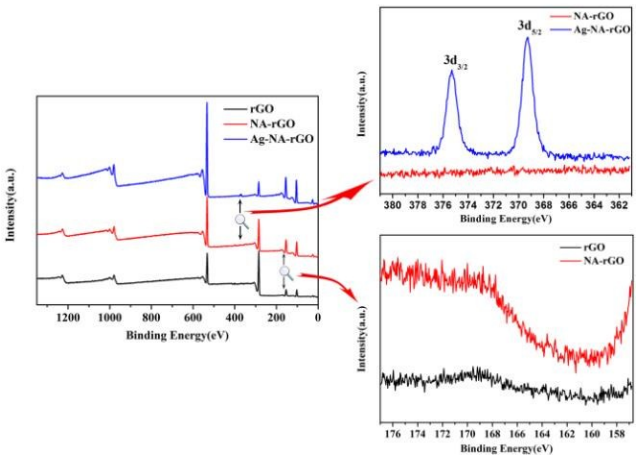


**Figure 4.** Typical XPS of prepared Ag-NA-rGO, NA-rGO and rGO materials

which showed the successive decrease of carbon because of the addition of new element in NA molecules and Ag nanoparticles.

The elemental composition of the prepared Ag-NA-rGO composite was further analyzed by energy dispersive spectroscopy (EDS) attached with TEM. Figure S2 shows the typical EDS spectrum of prepared Ag-NA-rGO composite which exhibited several well-defined peaks related with C, O, S and Ag. It is clear from the observed EDS spectrum that the majority of content in the prepared composite is carbon with the total percentage of 56.3%. The Ag content in the composite is 22.5%, which proves that Ag is available in the prepared composite. Further, the observed sulfur content in the prepared composite is 2.10%, which indicates the successful introduction of sulfophenyl groups via supramolecular interaction between NA and GO sheets.

### Sensibility of the Graphene-Based Gas Sensors

The sensitivity of multilevel graphene-based sensors is based on the used sensing materials and hence successive enhancements in the sensing responses were observed by the fabricated rGO, NA-rGO and Ag-NA-rGO based sensors. Chart S1 exhibits the ideal flow chart of gas sensing tests.

**Figure 5** illustrates the typical gas sensing responses of the rGO, NA-rGO and Ag-NA-rGO based sensors towards 10 ppm $NO_2$. Interestingly, the observed sensitivities for the fabricated

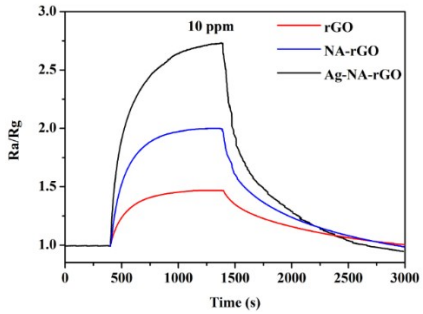


**Figure 5.** Typical gas sensing responses of rGO, NA-rGO and Ag-NA-rGO hybrid composites based sensors towards 10 ppm $NO_2$ gas.

gas sensors based on rGO, NA-rGO and Ag-NA-rGO hybrid composites were about 1.4, 2.0 and 2.8 times, respectively.

The sensitivities of the fabricated sensors are evaluated by the ratio of the initial and final resistance (Ra/Rg), recorded under air atmosphere and in presence of $NO_2$ gas, respectively. This can be expressed by the following equation:

$$S = \frac{R_{air}}{R_{gas}} = \frac{\dfrac{R_0}{-q \times \sum \iint_{xy} (p_{air} \times \mu_p \times \dfrac{d\zeta}{d\chi} + D_p \dfrac{dp}{d\chi}) dxdy} + R_c}{\dfrac{R_0}{-q \times \sum \iint_{xy} (p_{gas} \times \mu_p \times \dfrac{d\zeta}{d\chi} + D_p \dfrac{dp}{d\chi}) dxdy} + R_c}$$

as

$$p = \frac{n_i^2}{n} = n_i \exp\left(\frac{E_i - E_F}{KT}\right)$$

Where $R_0$ is a constant, $q$ is the quantity of electric charge, $p_{air}$ and $p_{gas}$ are the concentration of hole in air and $NO_2$ gas, respectively, $\sum \iint_{xy}$ is the total effective area, $\mu_p$ is the mobility of hole, $\zeta$ is the electric field intensity, $D_p$ is the diffusion coefficient of hole, $\chi$ is the distance, $R_c$ is the resistance from the films without sensing reaction, $n_i$ is a constant, n is the concentration of electron, $E_i$ and $E_F$ are the energy of the Fermi and the current material, K is the Boltzmann's constant, and $T$ is the temperature.

The hole conductivity occurs along with percolation paths via grain-to-grain contacts and therefore depends on the value of Schottky barrier of the adjacent grains[35, 36]. For Level I system in which rGO, a typical p-type semiconductor with holes as main carriers, was used (**Figure 6**, Level I). However, when the r-GO was functionalized with NA, the concentrations of holes ($P_{gas}$) of NA-rGO enhanced for the electronic absorption capacity of sulfophenyl groups in NA (Figure 6, Step 1, Level II). Besides, the oxidized gas ( $NO_2$) tends to absorb the lone-pair electrons on electron-rich sites such as S or O atoms in $SO_3^-$, NA-rGO would be further hole-doped ($P_{gas}$) for the improvement of electron-withdrawing ability of the sulfophenyl groups after $NO_2$ adsorption. Thus, the sensitivity of Level II enhanced significantly.

For Step 2, in Level III system in which Ag-NA-rGO hybrid composite was used (Figure 6, Level III)), the silver nanoparticles play very important role to isolate the graphene layers. The Ag nanoparticles segregate the graphene layers from a holistic entity into a multi-layer structure and hence permitting the penetration of $NO_2$ and the reaction with

interlayers, followed by the reduction in the resistance without sensing reactions ($R_c$). Meanwhile, the isolation of layers can also cause the decrease of $\chi$, namely, the increase of the change rate of electric field ($\frac{d\zeta}{d\chi}$), together with the increase of total effective area $\sum\iint_{xy}$. In addition, the gas adsorption ability of silver nanoparticles contributed the sensor to absorb extra $NO_2$ molecules which result the enhancement of the doping level ($P_{gas}$). Therefore, the sensitivity of fabricated gas sensor based on Level III system was further enhanced.

Apart from the superior response abilities, the fabricated sensors also showed good reversibility upon removing the adsorbed $NO_2$ molecules by switching to air (Figure 6). The results can be attributed to the weak combination between $NO_2$

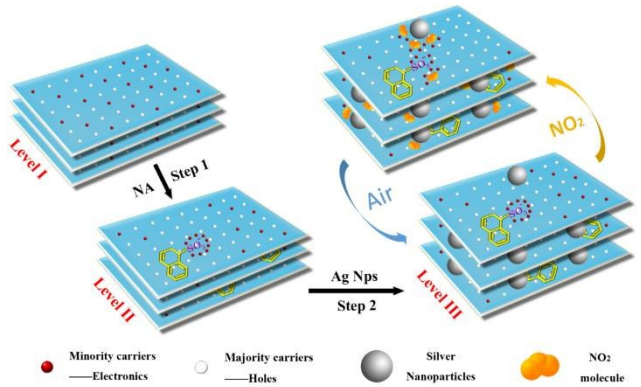


**Figure 6.** The ideal gas sensing mechanism for the gas sensors fabricated based on multilevel hybrid composites

molecules and lone-pair electrons in functional groups. Further, the isolation of graphene layers by silver nanoparticles led $NO_2$ molecules desorbed more easily.

Based on the above discussion, it is clear that the Level III system, i.e. Ag-NA-rGO hybrid composite, exhibited best sensing performance. Thus, to investigate the detailed sensing behavior and performances, the Ag-NA-rGO hybrid composite based sensor was examined under different concentrations of $NO_2$ gas and the observed results are shown in **Figure 7a**.

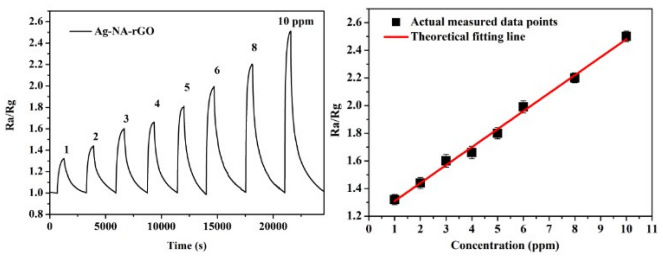


**Figure 7.** a) The responses of Ag-NA-rGO based sensor towards various concentrations of $NO_2$ gas (from 1ppm to 10 ppm), and b) the linear relationship with $NO_2$ concentration in the range of 1 to 10 ppm. The error bars for each measurement lie within the symbols themselves.

Interestingly, it was observed that with increasing the concentrations of $NO_2$ gas concentrations, from 1 ppm to 10 ppm, the Ra/Rg values increases significantly which revealed that the fabricated gas sensor is highly responsive toward both low and high concentrations of $NO_2$ gas and approximately 1.3 times of resistance change was observed after exposure to 1 ppm $NO_2$. Further, the detection limit of the fabricated Ag-NA-rGO hybrid composite based sensor was determined to be 1 ppm. The fabricated Ag-NA-rGO based sensor showed an outstanding linear detection range towards $NO_2$ with different concentrations from 1 ppm to 10 ppm and the sensitivity was measured from 1.3 to 2.5 times (**Figure 7b**). The observed results clearly demonstrate an important and facile approach to detecting low concentration of $NO_2$ for practical applications, thus the presented approach to fabricate $NO_2$ gas sensors can be applied for practical device applications.

To verify the reliable reproducibility and high stability of the fabricated sensing devices, the Ag-NA-rGO hybrid composite based sensor was exposed to 5 ppm $NO_2$ for three successive cycles and results are shown in **Figure 8a**. As evident from the observed results, that the fabricated sensor exhibited a stable response with an average sensitivity of 1.76 times. Moreover, the response time and recovery time of Ag-NA-rGO based sensor are 10 min and 40 min, respectively (Figure 8a). It is also important to mention that the sensitivity of the fabricated Ag-NA-rGO based sensor floats slightly within 5.6% of its initial value after 10-month aging process as demonstrated in Figure 8b. The observed results revealed that the fabricated Ag-NA-rGO hybrid composite based sensor exhibited very high stability which is one of the key factors in commercialized gas sensors.

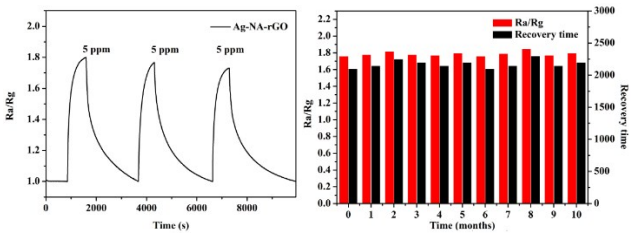


**Figure 8.** a) Reproducibility of Ag-NA-rGO hybrid composite based sensor exposed to 5 ppm $NO_2$ gas for three successive response cycles; and b) Stability of the fabricated Ag-NA-rGO based sensor after exposing it in air for 10 months.

The selectivity is one of the important characteristics for an efficient sensor; hence selectivity experiments were also performed for the fabricated Ag-NA-rGO based sensor. Several interfering gases such as acetone, ethanol, ammonia ($NH_3$) were used for the selectivity experiments. **Figure 9** exhibits the typical gas responses for the Ag-NA-rGO based sensor towards 10 ppm $NO_2$, acetone, ethanol and $NH_3$. From the observed selectivity results, interestingly, it was found that the fabricated Ag-NA-rGO based sensor exhibited excellent selectivity towards $NO_2$ gas compared to other used gases such as acetone, ethanol and $NH_3$. It was amazing to see that the sensing response towards 10 ppm acetone was only -1.44, while the selective response of $NO_2$ can reach over 40 times of acetone. The observed results confirmed that the fabricated sensor is highly selective towards $NO_2$ gas.

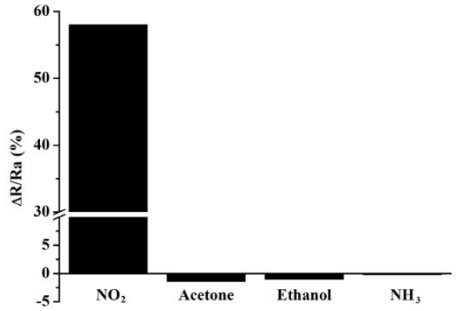


**Figure 9.** Selective responses of the fabricated Ag-NA-rGO based sensor towards 10 ppm $NO_2$, acetone, ethanol and $NH_3$.

## Experimental Section

The synthesis procedures for rGO, NA-rGO and Ag-NA-rGO were designed according to the reported literature.[16, 37, 38]

### Preparation of Graphene Oxide (GO)

GO was purchased from XianFeng NANO Co., Ltd. To disperse the GO into water, in a typical process, 100 mg of GO was put in 100 mL de-ionized (DI) water under vigorous ultrasonication for 30 min. After ultrasonication, a good suspension of GO can be obtained.

### Preparation of Reduced Graphene Oxide (rGO)

To prepare rGO, in a typical reaction process, 4 mL of GO dispersion, 16 mL of deionized water, 75 μL of ammonia (30%) and 10 mL of hydrazine hydrate (1.12 μL/mL) were mixed under sonication in a 50 mL round bottom flask. Consequently, the obtained mixture was then heated at 95 ℃ in an oil bath for 1 h to get stable rGO suspension.

### Preparation of Naphthalene-1-sulphonic acid sodium (NA) modified rGO (NA-rGO)

For preparing NA-rGO, typically 4 mL of GO dispersion was added in 10 mL of DI water to form a brown dispersion, followed by the addition of 92 mg of NA (Purchased from Alfa Aesar). Then, 5 mL of NaOH solution (4 mg/mL) was added dropwise to the dispersion, the mixture was finally kept at 80 ℃ for 1 h under stirring after the addition of 10 mL hydrazine hydrate. The reduced GO product was rinsed with water several times, and then re-dispersed in 20 mL of water under mild sonication.

### Preparation of Ag-NA-rGO composites

To prepare Ag-NA-rGO composite, 4 mL of GO dispersion was mixed with 10 mL of DI water in a 50 mL of round bottom flask under stirring until a uniform brown dispersion was formed. Consequently, 92 mg of NA and 16 mg of silver nitrate was added in the resultant solution. After addition of 5 mL of NaOH solution (4mg/mL) and 10 mL hydrazine hydrate, the mixture was further stirred for 1 h at 80 ℃ in an oil bath. Finally, the obtained mixture was rinsed with water for several times and Ag-NA-rGO suspension were obtained after the product re-dispersed in 20 mL of water by mild sonication.

### Fabrication of gas sensors based on rGO, NA-rGO and Ag-NA-rGO composites

To fabricated the gas sensors, interdigitated electrode (IE) were used which were made of alumina ceramic chips with platinum microelectrodes fixed in them (each electrode has 10 pairs of digits). All the sensors were fabricated through a Drop and Dry method. In a typical fabrication process, 0.1 mL of rGO/NA-rGO/Ag-NA-rGO dispersions (0.2 mg/mL) was dropped on the surface of IEs (10 pairs of digits with 5 μm fingers and 15 μm gaps, Synkera) and the coated IEs were dried on heating plate in air at 50 ℃ for 10 min. After the drying process, a thin layer of rGO, NA-rGO, and/or Ag-NA-rGO, respectively was formed on the IEs which were then connected by the Alligator clips for sensing tests.

### Sensing Tests

All the sensing tests were performed using a gas sensing system (CGS-1TP Intelligent Gas Sensing Analysis System, ELITE TECH. Chart S1). For all the gas sensing measurements a simple two-electrode configuration was employed. The sensitivities of the sensors were evaluated by measuring the changes in the resistances which were monitored by an automatic system. Prior to all gas sensing measurements, the gas cylinder was purged with pure air gas and after achieving a constant resistance, the fabricated sensors were sequentially exposed to $NO_2$ and air at room temperature (25 ℃) in the range of 40−70% relative humidity (RH). To check the reproducibility, all sensors were fabricated at least 3 times and characterized in terms of their sensing performances and finally the average values are reported.

### Characterizations of rGO, NA-rGO and Ag-NA-rGO composites

The prepared sensing materials were characterized by several techniques. The surface morphology of the prepared Ag-NA-rGO composite was examined by atomic force microscopy (AFM; Dimension Icon instrument (USA)). The detailed structural properties of the prepared materials were examined by Raman-scattering spectroscopy (HORIBA Jobin Yvon Raman microscope (LabRAM HR800)) measured with a 514 nm laser at a power density of 4.7 mW. The surface properties were examined by X-ray photoelectron spectra (XPS; ESCALAB 250 photoelectron spectrometer (ThermoFisher Scientific, USA)). The general morphologies of the prepared materials were examined by SEM (Quanta 250 FEG, FEI) and TEM microscopes (Sirion-200, Japan). All the conductivity measurements were done by conventional four-probe technique.

## Conclusions

In summary, a multilevel supramolecular structure composed of NA and silver nanoparticles on rGO composite (Ag-NA-rGO) was prepared and used for the fabrication of highly sensitive and selective $NO_2$ gas sensor. Interestingly, with the supramolecular modification, the water-solubility of Ag-NA-rGO was greatly improved for the hydrophilicity of sulfophenyl groups in NA. Besides, the fabricated sensors tend to be hole-doped due to the electron withdrawing ability of NA which results in the improvement of sensitivities of the fabricated sensors. In addition, by introducing silver nanoparticles in Ag-NA-rGO composite, the inherent ability to capture gaseous molecules and specific surface area was increased. The silver nanoparticles play a key role in the isolation of graphene layers and segregate the graphene layers from a holistic entity to a multi-layer structure which permits the penetration of $NO_2$ and the reaction with interlayers cause significant improvement in



 

the sensitivities of the fabricated Ag-NA-rGO based sensors. Moreover, the isolation of layers by silver nanoparticles provides enough space for gas desorption, which is beneficial to the reversibility. Compared with conventional graphene-based sensors, the multilevel Ag-NA-rGO-based sensors exhibited over 2.8 times greater response towards 10 ppm $NO_2$ and the sensing signals increases linearly in the concentration range of 1 ppm to 10 ppm. The presented work demonstrates a possibility to fabricate highly sensitive, reproducible, stable and selective gas sensors based on supramolecularly modified graphene.

## Acknowledgements

This work was supported by the National Natural Science Foundation of China (Grant No.51373005) Program for New Century Excellent Talents in University (NCET-10-0035), National Key Basic Research Program of China (2014CB931800).

## Notes and references

[a] Key Laboratory of Bio-Inspired Smart Interfacial Science and Technology of Ministry of Education, School of Chemistry and Environment, Beihang University, Beijing 100191, P R China.
[b] Department of Chemistry, Faculty of Science and Arts and Promising Centre for Sensors and Electronic Devices, Najran University, Najran 11001, P.O.Box-1988, Kingdom of Saudi Arabia
[c] Gas and Humidity Sensing Department, Beijing Elite Tech Co., Beijing 100850, PR China
[d] Beijing National Laboratory for Molecular Sciences(MNLMS), Key Laboratory of Organic Solid, Institute of Chemistry, Chinese Academy of Sciences, Beijing 100190, China

Electronic Supplementary Information (ESI) available. See DOI: 10.1039/b000000x/

1. K. S. Novoselov, A. K. Geim, S. Morozov, D. Jiang, Y. Zhang, S. Dubonos, I. Grigorieva and A. Firsov, *Science*, 2004, **306,** 666.
2. Y. Zhang, Y.-W. Tan, H. L. Stormer and P. Kim, *Nature*, 2005, **438,** 201.
3. F. Schedin, A. Geim, S. Morozov, E. Hill, P. Blake, M. Katsnelson and K. Novoselov, *Nature Mater.*, 2007, **6,** 652.
4. Q. Cheng, M. Wu, M. Li, L. Jiang and Z. Tang, *Angew. Chem., Int. Ed.* 2013, **125,** 3838.
5. X. Li, X. Wang, L. Zhang, S. Lee and H. Dai, *Science*, 2008, **319,** 1229.
6. S. Stankovich, D. A. Dikin, G. H. Dommett, K. M. Kohlhaas, E. J. Zimney, E. A. Stach, R. D. Piner, S. T. Nguyen and R. S. Ruoff, *Nature*, 2006, **442,** 282.
7. S. Watcharotone, D. A. Dikin, S. Stankovich, R. Piner, I. Jung, G. H. Dommett, G. Evmenenko, S.-E. Wu, S.-F. Chen and C.-P. Liu, *Nano Lett.*, 2007, **7,** 1888.
8. T. Ramanathan, A. Abdala, S. Stankovich, D. Dikin, M. Herrera-Alonso, R. Piner, D. Adamson, H. Schniepp, X. Chen and R. Ruoff, *Nat. Nanotechnol*, 2008, **3,** 327.
9. X. Du, I. Skachko, A. Barker and E. Y. Andrei, *Nat. Nanotechnol*, 2008, **3,** 491.
10. D. Chen, H. Feng and J. Li, *Chem. Rev.*, 2012, **112,** 6027.
11. F. Yavari and N. Koratkar, *J. Phys. Chem. Lett.*, 2012, **3,** 1746.
12. Y. Ju âYun, H. Ju âPark, S. Eon âMoon and B. Hoon âKim, *Nanoscale*, 2014, **6,** 6511.
13. Y. Yang, C. Tian, J. Wang, L. Sun, K. Shi, W. Zhou and H. Fu, *Nanoscale*, 2014, **6,** 7369.
14. Q. He, S. Wu, Z. Yin and H. Zhang, *Chem. Sci.*, 2012, **3,** 1764.
15. A. Lipatov, A. Varezhnikov, P. Wilson, V. Sysoev, A. Kolmakov and A. Sinitskii, *Nanoscale*, 2013, **5,** 5426.
16. D. Li, M. B. Müller, S. Gilje, R. B. Kaner and G. G. Wallace, *Nat. Nanotechnol*, 2008, **3,** 101.
17. Y. Hernandez, V. Nicolosi, M. Lotya, F. M. Blighe, Z. Sun, S. De, I. McGovern, B. Holland, M. Byrne and Y. K. Gun'Ko, *Nat. Nanotechnol*, 2008, **3,** 563.
18. I. Jung, D. A. Dikin, R. D. Piner and R. S. Ruoff, *Nano Lett.*, 2008, **8,** 4283.
19. W. Yuan, A. Liu, L. Huang, C. Li and G. Shi, *Adv. Mater.*, 2013, **25,** 766.
20. S. Srinivasan, S. H. Je, S. Back, G. Barin, O. Buyukcakir, R. Guliyev, Y. Jung and A. Coskun, *Adv. Mater.*, 2014, **26,** 2725.
21. H.-W. Yu, H. K. Kim, T. Kim, K. M. Bae, S. M. Seo, J.-M. Kim, T. J. Kang and Y. H. Kim, *Acs Appl. Mater. Interfaces*, 2014, **6,** 8320.
22. H. Zhang, J. Feng, T. Fei, S. Liu and T. Zhang, *Sensor Actuat. B-chem*, 2014, **190**, 472.
23. W. Li, Y. Kim and M. Lee, *Nanoscale*, 2013, **5,** 7711.
24. T. Aida, E. Meijer and S. Stupp, *Science*, 2012, **335,** 813.
25. E. Busseron, Y. Ruff, E. Moulin and N. Giuseppone, *Nanoscale*, 2013, **5,** 7098.
26. Q. Zhou, Y. Li, Q. Li, Y. Wang, Y. Yang, Y. Fang and C. Wang, *Nanoscale*, 2014, **6,** 8387.
27. S. Liu, B. Yu, H. Zhang, T. Fei and T. Zhang, *Sensor Actuat. B-chem*, 2014, **202**, 272.
28. L. Huang, Z. Wang, J. Zhang, J. Pu, Y. Lin, S. Xu, L. Shen, Q. Chen and W. Shi, *Acs Appl. Mater. Interfaces*, 2014, **6,** 7426.
29. Y. H. Su, Y. K. Wu, S. L. Tu and S.-J. Chang, *Appl. Phys. Lett.*, 2011, **99,** 163102.
30. W. Zhang, F. Li, Y. Hu, S. Gan, D. Han, Q. Zhang and L. Niu, *J. Mater. Chem. B*, 2014, **2,** 3142.
31. Q. Su, S. Pang, V. Alijani, C. Li, X. Feng and K. Müllen, *Adv. Mater.*, 2009, **21,** 3191.
32. Y. Q. Li, T. Yu, T. Y. Yang, L. X. Zheng and K. Liao, *Adv. Mater.*, 2012, **24,** 3426.
33. W. Shao, X. Liu, H. Min, G. Dong, Q. Feng and S. Zuo, *Acs Appl. Mater. Interfaces*, 2015, **7,**6966.
34. P. Bazant, I. Kuritka, L. Munster and L. Kalina, *Cellulose*, 2015, **22,** 1275.
35. M. E. Franke, T. J. Koplin and U. Simon, *Small*, 2006, **2,** 36.

36. N. Barsan, D. Koziej and U. Weimar, *Sensor Actuat. B-chem*, 2007, **121,** 18.
37. J. Che, L. Shen and Y. Xiao, *J. Mater. Chem*, 2010, **20,** 1722.
38. Y. Si and E. T. Samulski, *Nano Lett.*, 2008, **8,** 1679.



 